STUDY OF SEPARATION DYNAMICS AND SYSTEMS RELATED TO STAGING OF ATLAS-CENTAUR

by Richard W. Heath, Henry Synor, Ralph F. Schmiedlin,

and John H. Povolny

Lewis Research Center
Cleveland, Ohio

NATIONAL AERONAUTICS AND SPACE ADMINISTRATION

STUDY OF SEPARATION DYNAMICS AND SYSTEMS RELATED TO STAGING OF ATLAS-CENTAUR

By Richard W. Heath, Henry Synor, Ralph F. Schmiedlin, and John H. Povolny

Lewis Research Center
National Aeronautics and Space Administration
Cleveland, Ohio

E-3700

SUMMARY

A series of tests was performed on a full-scale model of the Atlas-Centaur vehicle in a test chamber at the Lewis Research Center to obtain information concerning the dynamic behavior of the two stages during the separation time interval. At the same time, data were obtained relating to the reliability of the various systems involved in the staging process.

The test article motions, in general, conformed to those predicted by dynamics equations, in that the direction of movement observed was the same as that indicated by the dynamics equations, but the magnitude of motion did not agree precisely. As a result of this test series, it was concluded that satisfactory staging of the Atlas from the Centaur will occur, even if one of the eight retrorockets does not fire.

The linear-shaped charge, which cuts the interstage adapter during the separating sequence, successfully functioned in every test. The detonating train serving the shaped charge performed satisfactorily with the exception of marginal behavior noted in the functioning of a "safe and arm device" used to initiate the detonation.

The retrorocket system produced difficulties in that a number of misfires were encountered. The need for an improved igniter was indicated and a new design was obtained.

TM X-52292

INTRODUCTION

The Atlas-Centaur staging system consists essentially of two subsystems: a linear-shaped charge and a retrorocket system. The linear-shaped charge severs the interstage adapter at its forward end to separate the two vehicles and the retrorockets decelerate the Atlas away from the Centaur at approximately 1/2 g. This approach was used to minimize uncertainties arising from ice bonding at the separation plane, which is thermally close to the cold liquid-hydrogen - liquid-oxygen (LH_2/LO_2) Centaur propellant tank, and to minimize the time interval involved in the staging process.

An analysis by the General Dynamics/Convair Division indicated that (1) there would be only minor disturbances imparted to the vehicles, and (2) there was enough safety margin to avoid collision in the event of a retrorocket failure. To verify those predictions, an experimental investigation was conducted with a full-scale model (to eliminate scaling effects), using flight hardware where feasible and operating in an evacuated chamber to duplicate rocket thrust and expansion effects and to eliminate the damping effects of the atmosphere. A converted wind tunnel at the Lewis Research Center was utilized for this investigation because of its large internal volume that enabled it to contain full-scale mockups and maintain a moderate vacuum throughout the rocket firing.

While the primary test objective was the evaluation of flight dynamics, consideration was also given to obtaining performance information on the various systems associated with the staging operation. The several tests performed with (1) the linear-shaped charge, (2) the shaped charge train, (3) the retrorockets, and (4) the firing relay assembly were expected to shed considerable light on the reliability of these systems.

APPARATUS

Part of the existing altitude wind tunnel was converted to an altitude chamber by the removal of its propeller, turning vanes, and heat-exchanger apparatus and by the eroection of bulkheads at its southeast corner and at its test bed section. As a result, a chamber was formed with a test section 121 feet (37m) long and 51 feet (15.6m) in diameter with adjoining legs. The volume of the entire chamber, including the test section and the adjacent legs, is of the order of 600,000 cubic feet (17,000 m^3). To reduce the likelihood of recirculating rocket exhaust gas being directed by one of the chamber legs and impinging on the model, the main chamber wall was extended to separate the test area from this leg. This extension was accomplished by constructing a tarpaulin barrier on a cable frame across the end of the adjoining leg. A plan view of the converted chamber is shown in figure 1. The chamber was joined to the laboratory central exhaust system, which is capable of providing a vacuum equivalent to that of approximately 100,000 feet (30500m) altitude.

A suspension system was built into the roof of the test section. It included a dual rail trolley and hoist from which the Atlas was hung (fig. 2). The trolley from which the Atlas was suspended was accelerated by a system of weights that were released at the same moment that the retrorockets were fired. The weights were arrested in their travel at a time corresponding to rocket burnout, and the trolley was propelled through the balance of its travel by a coast weight sized to overcome frictional drag. Changes in Atlas acceleration caused by firing different numbers of retrorockets were compensated for by varying the weights propelling the trolley. The Centaur model was suspended from a fixed point, as it was anticipated that its motion during the time interval of interest would be quite small due to its large weight of 38,000 pounds (17,200 kg).

The Atlas model simulated the flight booster's external dimensions. The weight, which was approximately 10,000 pounds (4540 kg), the center of gravity location, and the moments of inertia at the time of separation were duplicated as closely as possible. The Atlas framework consisted of a skeleton framework of ribs and braces. The retrorocket locations on the Atlas duplicated their flight configuration positions, and forms simulating Atlas pods and vernier engine fairings were mounted to provide a realistic environment for the retrorocket gases, as shown in figure 3. An overall view of the Atlas model as used in the tests is shown in figure 4.

The test-article interstage adapter was modified by replacing the forward end with an expendable 2-foot-long (0.6-m-long) section. This expendable section permitted the replacement of a small, easily handled unit after cutting by the shaped charge rather than replacing the whole adapter (fig. 5).

The Centaur vehicle was represented by a Centaur liquid-oxygen tank supported by a stainless-steel enclosure with weight-bearing outrigger arms attached (fig. 6). The arms were used for positioning and holding lead weights that were sized and placed so as to duplicate the flight vehicle mass and moments of inertia at the time of staging. Aft of the tank a fiber glass "clearance envelope" was affixed, as seen in figure 7, representing a boundary that encompassed all articles of hardware (engines, helium and hydrogen peroxide bottles) normally mounted on the Centaur's rear bulkhead. The use of the clearance envelope provided a visible reference that indicated the degree of allowable motion of the two vehicles relative to one another. References marks on the envelope provided an aid in determining the magnitude of the relative motion observed.

At the termination of the Atlas' longitudinal travel, it was arrested by a vertical net erected at the end of the chamber. The arresting hooks on the Atlas framework that engaged the net and prevented rebounding are shown in figure 8.

The Atlas was suspended by a gimbal and swivel joint at its center of gravity, which allowed freedom of motion in pitch, yaw, and roll. Lateral translation was limited to the small amount allowed by pendulous motion through the suspension cable. The foregoing freedoms of motion, plus the freedom of longitudinal motion allowed by the trolley travel, provided five degrees of freedom for the Atlas in these tests.

The Centaur was suspended by a yoke and swivel joint that allowed freedom of motion in pitch and yaw. Freedom of longitudinal and lateral translations was limited to that allowed by pendulous motion through the Centaur suspension cable. Thus, the Centaur mockup was permitted four degrees of freedom through small motions. The suspension joint is shown in figure 6.

Vehicle motions were recorded by high-speed motion-picture cameras and motion transducers which consisted of (1) flight-type rate gyros, (2) accelerometers, and (3) extensometers. The locations of these devices are shown in figure 9.

Two model configurations were used in the test series. The first configuration was similar to the second Centaur flight (AC-2). The second configuration simulated the sixth flight (AC-6) and included a lighter interstage adapter, which caused changes in the center of gravity and the moment of inertia. Also, the shaped-charge detonator and initiation train were simplified. The AC-6 detonator, which replaced the safe and arm device, is shown in figure 10, and a portion of the detonation transfer train is shown in figure 11. The

steel plates, which served as adapter guides during the first separation motions on AC-2, were replaced by fiber glass "bumpers" on AC-6. The retrorockets, with the exception of their igniters, and the shaped charge were unchanged.

The mechanism used to sever the interstage adapter was a linear-shaped charge assembly made of cyclotrimethylene trinitramine (RDX) contained in a lead sheath shaped and positioned to locally amplify the explosive force in a narrow band against the adapter. The charge was ignited, in the case of the AC-2 configuration, by a detonator mounted integrally with an electromechanical safe and arm device. For the AC-6 configuration, instead of a safe and arm device, a detonator was used which employed a 1-ampere - 1-watt no-fire initiator to prevent inadvertent firing.

PROCEDURE

Before each test the two mockups were bolted together, the interstage adapter was fitted with a linear-shaped charge, and either seven or eight live retrorockets were installed. A number of tests were performed with seven rockets installed, the eighth rocket being simulated by a mass dummy to represent a failed motor. The mass dummy was located in the position expected to create the greatest torque imbalance and the most angular motion on the part of the Atlas. The Atlas supporting trolley was held in place by means of an explosive bolt and the mated vehicles were raised to a position with their centerlines 20 feet (6.1m) above the chamber floor, 5 feet (1.5m) below the chamber center, to minimize the effects of recirculating gas impingement. Accelerating weights were attached to the trolley system in amounts required to match the anticipated Atlas acceleration as it varied with the use of either seven or eight retrorockets.

During a test run, the chamber was evacuated to a pressure equivalent to approximately 100,000 feet (30,500m) in altitude. The recording oscillographs were then operated at high speed and the motion-picture cameras were turned on by command from the test programmer so that all equipment would be up to speed by the time the pyrotechnics were detonated. The programmer then fired the shaped charge and, after a 1/10-second time delay (as is in flight), the trolley release bolt and the retrorockets were fired simultaneously. A typical rocket firing sequence is shown in figure 12.

Following each run, the motion picture and oscillograph records were reduced manually and converted to curve form. Rocket pressure-time tabulations were made and, by the use of a pressure-thrust relation, converted to thrust against time. Integration of the area under each curve gave the total impulse imparted to the vehicle. The accuracy of the pressure-thrust relation was verified by simultaneously monitoring the chamber pressure and actual thrust of a rocket as measured by a strain gage on a mounting fixture.

Longitudinal extensometer and photographic data were compared to give an indication of the Atlas' displacement against time. The derivative of the resulting plot was averaged with the accelerometer data to determine the Atlas acceleration, and this information was compared with the computed rocket impulse to determine the magnitude of any thrust losses.

Atlas rate gyro data were double integrated to obtain an indication of angular motion of the interstage adapter. Lateral translation of the Atlas model, including the interstage adapter, was determined by photographic means, and thus the total lateral motion of the adapter was obtained from both angular and translational components. This information was compared with photographic

data to arrive at the indicated motion of the adapter forward end (station 413) during separation. Observed Atlas behavior during separation was compared with analytical predictions.

By means of extensometers and rate gyros, it was similarly possible to determine the Centaur's motion at the same time.

Malfunctions of components vital to the separation process were examined and steps were taken to increase the reliability of these components.

RESULTS AND DISCUSSION

Dynamics Studies

The Atlas retarding rockets are assymetrically located about the vehicle's pitch axis to partly compensate for the center of gravity offset from its centerline and to thus minimize the moment imbalance about this axis during retro firing (fig. 13).

Inasmuch as the location of the center of gravity is affected by the amount and location of residual fuels, it will vary from flight to flight; an exact compensation cannot be attained by means of rocket placement, but a best compromise is effected. The model configuration during test 1, as noted in table I, simulated the estimated AC-2 center-of-gravity location, and the subsequent model configuration simulated the AC-6 center-of-gravity location. Differences in predicted motions between the two can largely be attributed to the differences in the center-of-gravity locations. Some of the difference is due to changes in the vehicle mass and moments of inertia that result from a change in the interstage adapter weight.

It was found, during the rocket-thrust-against-pressure study on the static firing stand, that the retrorockets generated approximately 500 pound-seconds (2240n-sec.) of impulse, which was their nominal rating. The Atlas

acceleration data, however, indicated a net impulse of approximately 400 pound-seconds (1790 n-sec.) under the same test conditions. Since there were no exterior restraining forces, it is concluded that the 20-percent impulse loss is the result of Atlas skin friction. (The net thrust realized was used in calculating motion predictions.)

The motions observed during tests in which all rockets were fired are tabulated and compared (table I) with predictions based on equations developed in reference 1. A sample calculation of predicted motion using these equations is shown in the appendix. The actual model motions consistently exceeded predictions, with the average terminal displacement being 2.5 inches (6.35 cm) greater than predicted along the pitch axis and 1.4 inches (3.56 cm) greater than predicted along the yaw axis. While the observed motions exceed the predicted, the magnitude of the difference is not great. It appears that lateral displacements may be calculated closely by the use of the equations noted in reference 1.

The clearance between the adapter and the Centaur hardware is represented by the "clearance envelope" (fig. 7). Profile views of the hardware-controlling boundary of the envelope are shown in figures 14 and 15. The terminal separation occurs after 108 inches (274 cm) of longitudinal motion of the Atlas. The minimum clearance remaining after the largest pitch displacement of the interstage adapter, resulting from eight rockets firing, was approximately 9.6 inches (24.4 cm), as seen in figure 14. This clearance is considered to be sufficiently large to absorb any reasonable anomalies that might occur in later tests or in flight.

To observe the model behavior with a single rocket failure, some of the tests were conducted with rocket 1 not operating, which analysis showed to be the worst case. The predicted and observed results are presented in table II and are in close agreement. Comparison of available clearance with the observed motion indicates that the failure of one rocket will not cause collision.

Figures 14 and 15 also show the adapter motions and the clearances between the two stages, the pitch and yaw planes, for both seven and eight rockets firing. The worst case observed is shown in both figures.

Systems Function Studies

It was found that, in the 18 firings accomplished, the linear-shaped charges consistently produced a clean cut through the metal at all locations. A typical cut section is shown in figure 16. The safe and arm devices presented a problem in that occasionally their mechanical arming mechanism failed to operate properly and prevented detonation. The device was subsequently replaced by the AC-6 detonator which did not incorporate the moving element and circumvented the arming problem. Difficulties of another type occurred with the new detonator in that it fractured its mounting bolts when fired and presented a potential shrapnel problem (fig. 10). The mounting was redesigned to correct this problem.

During the series of tests, the retrorockets occasionally failed to ignite even though their igniters successfully fired. Investigation revealed that the igniters were inadequate, and a new igniter was subsequently used on Atlas-Centaur flights (ref. 2). The new igniter was used in the balance of the test series and produced no misfires.

Various ancillary items of equipment also exhibited occasional performance malfunction. In one instance, the electrical staging disconnect plug failed to

respond to its eject signal prior to separation; it parted in response to its mechanical backup lanyard pull. Subsequently, the time interval between the issuance of the electrical signal and vehicle staging was lengthened to allow sufficient time for ejection of the plug by its primary means, the electrical signal. Also, the lanyard attachment was modified to prevent cocking and to relieve frictional stresses during separation.

Four plastic helium chill-down ducts, serving the engine ground chill operation, were installed on the test vehicle to evaluate their disconnecting characteristics. It was found that they consistently parted by tearing a weak-link section rather than by sliding apart at a slip-joint connection located at the engine, which was designed to be the primary disconnecting point. A view of one of the ducts with a parted weak link is shown in figure 17. This method of parting was not considered to be detrimental to flight performance but, subsequently, the primary joint was redesigned.

In flight the retrorockets are covered by aerodynamic fairings with blow-off end caps. The caps have tear-away tabs designed to cause the caps to be ejected at an angle from the Atlas and prevent possible impingement on the vehicle. Several fairings were tested for proper operation on some of the separation tests. It was found that, occasionally, the caps would not tear off, as seen in figure 18. Caps remaining on the fairing could potentially interfere with the rocket exhaust; consequently, the tear-away tabs were redesigned.

Prior to staging, the insulation panels were cut from their lower attachment point by a linear-shaped charge similar to the one on the interstage adapter. The two charges are located approximately 1.25 inches (3.18 cm) from one another, with the possibility that the firing of the panel charge could have deleterious

effects on the staging charge. On two occasions the two charges were mounted, as in flight, and the panel charge was fired prior to the staging charge. No cross effects were observed.

CONCLUSIONS

The Atlas-Centaur staging system, in its final flight configuration, provides for satisfactory separation of the stages. The retarding-rocket placement geometry allows for a malfunction of any one rocket without the probability of a collision between the stages.

The test series indicated that the linear-shaped charge as used on the Atlas-Centaur vehicle will perform reliably to effect a mechanical stage separation. The retarding rockets, while originally subject to erratic ignition, have been improved and now operate satisfactorily.

APPENDIX

Sample Calculation of Predicted Motion

The derivation of the equation generated by General Dynamics/Convair for the prediction of separation dynamics is presented in reference 1. The equation, as used in the separation tests, is

$$S_Z = - \frac{m \ell R}{I_{yy}} \left\{ - S_X + \frac{1}{m} \left[-n \int_0^{t_o} (t_x - \tau)\, F(\tau)\, d\tau \right] \right\} \frac{1}{n} \sum_{i=i}^{n} \left(\sin \varphi_i + \frac{\overline{Z}}{R} \right)$$

and is designed for general applications.

Symbols used in the following analyses are defined as follows:

F average thrust characteristic for single retrorocket, lb (kg)

I_{yy}, I_{zz} moment of inertia of booster vehicle about transverse axes through center of gravity, slug-ft^2 (kg-m^2)

ℓ vector from center of gravity of booster vehicle to forward end of interstage adapter in x-, y- , z-reference frame, ft (m)

m mass of booster vehicle, slug (kg)

n number of retrorockets, nondimensional

R distance from centerline of booster vehicle to center of retrorocket exit nozzle, ft (m)

S_x relative axial separation distance, ft (m)

S_z lateral clearance used (z-component as seen by an observer whose reference frame is x, y, z), ft (m)

t_o time to clear separation guides, sec

t_x total time to clear Centaur engines, sec

$\overline{Z}$ offset of Atlas center of gravity from its centerline along Z-axis, ft (m)

φ_i angle defining angular location i^{th} retrorocket, deg

τ dummy variable used for time, sec

A sample calculation for motion in one plane follows. A set of parameters applying to eight rockets firing are

$$S_z = -\frac{m\ell R}{I_{yy}} \left\{ -S_x + \frac{1}{m} \left[-n \int_0^{t_o} (t_x - \tau)\, F(\tau)\, d\tau \right] \right\} \frac{1}{n} \sum_{i=1}^{n} \left(\sin \varphi_i + \frac{\bar{Z}}{R} \right)$$

$$= -\frac{m\ell R}{nI_{yy}} \left\{ -S_x + \frac{1}{m} \left[-n F \frac{1}{2} (2\, t_o\, t_x - t_o)^2 \right] \right\} \left(\frac{n\bar{Z}}{R} + \sum_{i=1}^{n} \sin \varphi_i \right)$$

where

F = 550 lb (250kg)

I_{yy} = 107 300 slug-ft^2 (145 500 kg-m^2)

ℓ = 45.5 ft (13.9m)

M = 303 slugs (440kg)

n = 8 rockets

R = 5.25 ft (1.6 m)

S_x = -9 ft (-2.74 m)

t_o = 0.339 sec, time to clear guide bumpers

t_x = 1.32 sec, time to clear Centaur

$\sum_{i=1}^{n} \sin \varphi_i = 0.678$

$\bar{Z}$ = -0.9 ft (-0.27 m)

Substituting these values gives

$$S_z = -\frac{303\ (45.5)\ 5.25}{8\ (107\ 300)} \left\{ +9 + \frac{1}{303} \left[\frac{-8\ (550)}{2} \left(2 \cdot 0.339 \cdot 1.32 - 0.339^2 \right) \right] \right\}$$

$$\left(\frac{8\ (-0.9)}{5.25} + 0.678 \right) = 0.195 \text{ ft } (0.0595 \text{ m})$$

$S_z = 2.34 \approx 2.3$ in. (5.84 cm) (equivalent to 2.3 in. (5.84 cm) pitch down)

Computing for motion in the perpendicular plane yields

$$S_y = -\frac{m\ell R}{nI_{zz}} \left\{ -S_x + \frac{1}{m} \left[-n F \frac{l}{2} (2 t_o t_x - t_o^2) \right] \right\} \left(\frac{n\bar{Y}}{R} + \sum_{i=1}^{n} \cos \varphi_i \right)$$

Substituting

I_{zz} = 107 381 slug-ft^2 (145,900 kg-m^2)

$\bar{Y}$ = -0.342 ft (-0.104 m)

$$\sum_{i=1}^{n} \cos \varphi_i = 0$$

in the preceding S_y equation yields

$$S_y = -0.0843 \left\{ 3.34 \right\} \left[\frac{8 (-0.342)}{5.25} + 0 \right]$$

= 0.147 ft (0.0448 m)

= 1.8 in. (4.57 cm) (equivalent to 1.8 inches (4.57 cm) yaw right)

REFERENCES

1. Anon.: Flight Dynamics and Control Analysis of the Centaur Vehicle (Atlas/Centaur AC-4). Rep. No. GD/A-DDE64-077, General Dynamics/Astronautics, Oct. 1964.

2. Heath, Richard W., Synor, Henry, Schmiedlin, Ralph F., and Povolny, John H.: Investigation of Atlas Solid Fuel Retarding Rocket During Atlas/Centaur Separation Tests. NASA TM X-1119, 1965.

TABLE I. - ALL ROCKETS FIRED
Predicted motions were computed by means of
General Dynamics/Convair equation shown in the appendix.

Test	Pitch motion of station 413				Yaw motion of station 413			
	Predicted,		Observed,		Predicted,		Observed,	
	in.	(cm)	in.	(cm)	in.	(cm)	in.	(cm)
[a]1	2.0	(5.1)	3.5	(8.9)	2.2	(5.6)	4.0	(10.2)
2	2.8	(7.1)	3.9	(9.9)	2.1	(5.3)	5.8	(14.7)
3	2.8	(7.1)	4.9	(12.5)	2.1	(5.3)	4.5	(11.4)
4	2.8	(7.1)	3.2	(8.1)	2.1	(5.3)	3.7	(9.4)
5	2.8	(7.1)	4.5	(11.4)	2.1	(5.3)	5.2	(13.2)

[a]Note: Test 1 simulated the AC-2 flight configuration; the balance of the tests simulated the AC-6 configuration.

TABLE II. - ROCKET 1 NOT FIRED
Predicted motions were computed by means of
General Dynamics/Convair equation shown in the appendix.

Test	Pitch motion of station 413				Yaw motion of station 413			
	Predicted,		Observed,		Predicted,		Observed,	
	in.	(cm)	in.	(cm)	in.	(cm)	in.	(cm)
6	6.0	(15.2)	6.2	(15.8)	---	---	---	---
7	6.0	(15.2)	8.3	(21.1)	0.3	(0.8)	0.8	(2.0)

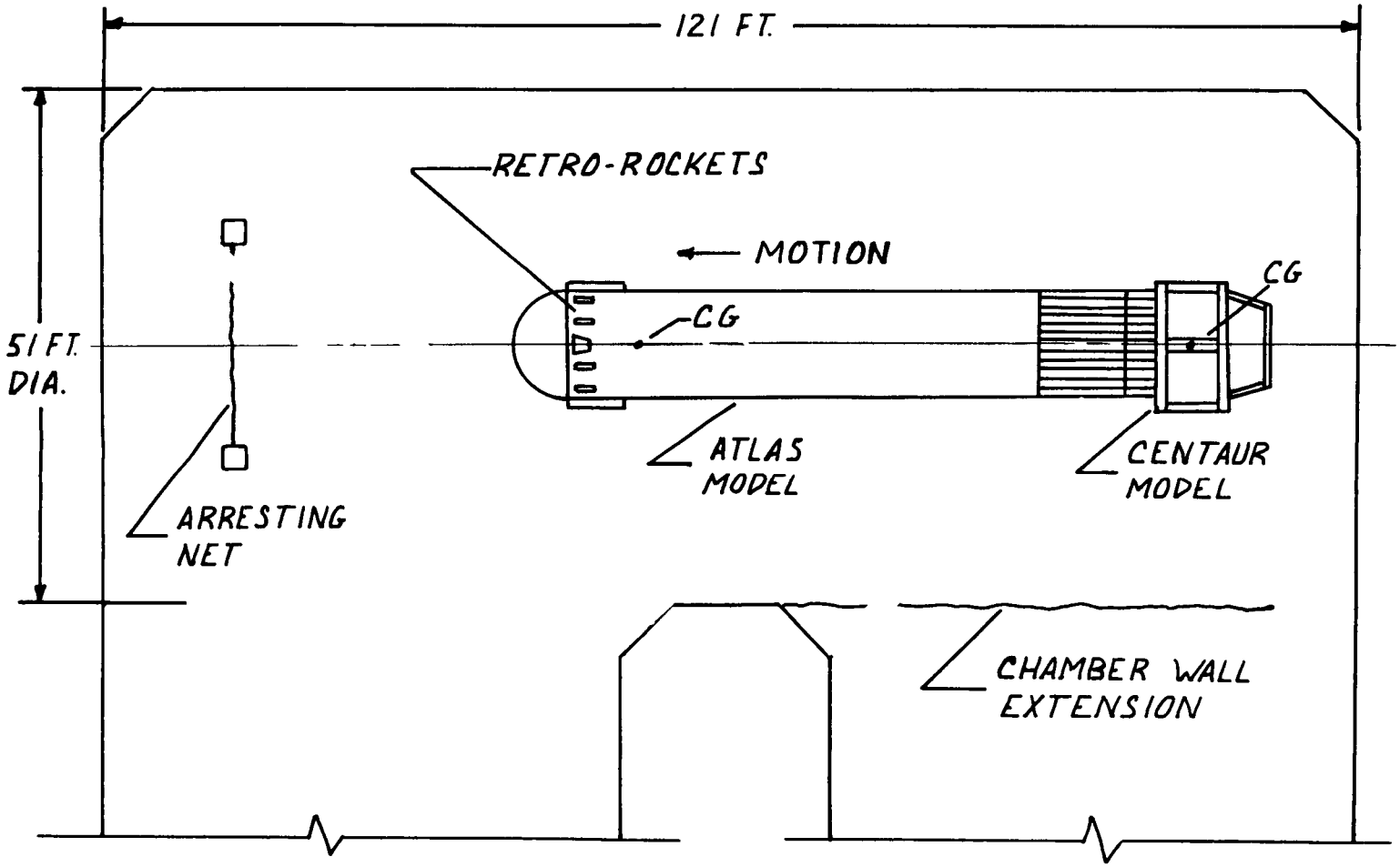

FIGURE 1. PLAN VIEW OF SEPARATION TEST CHAMBER

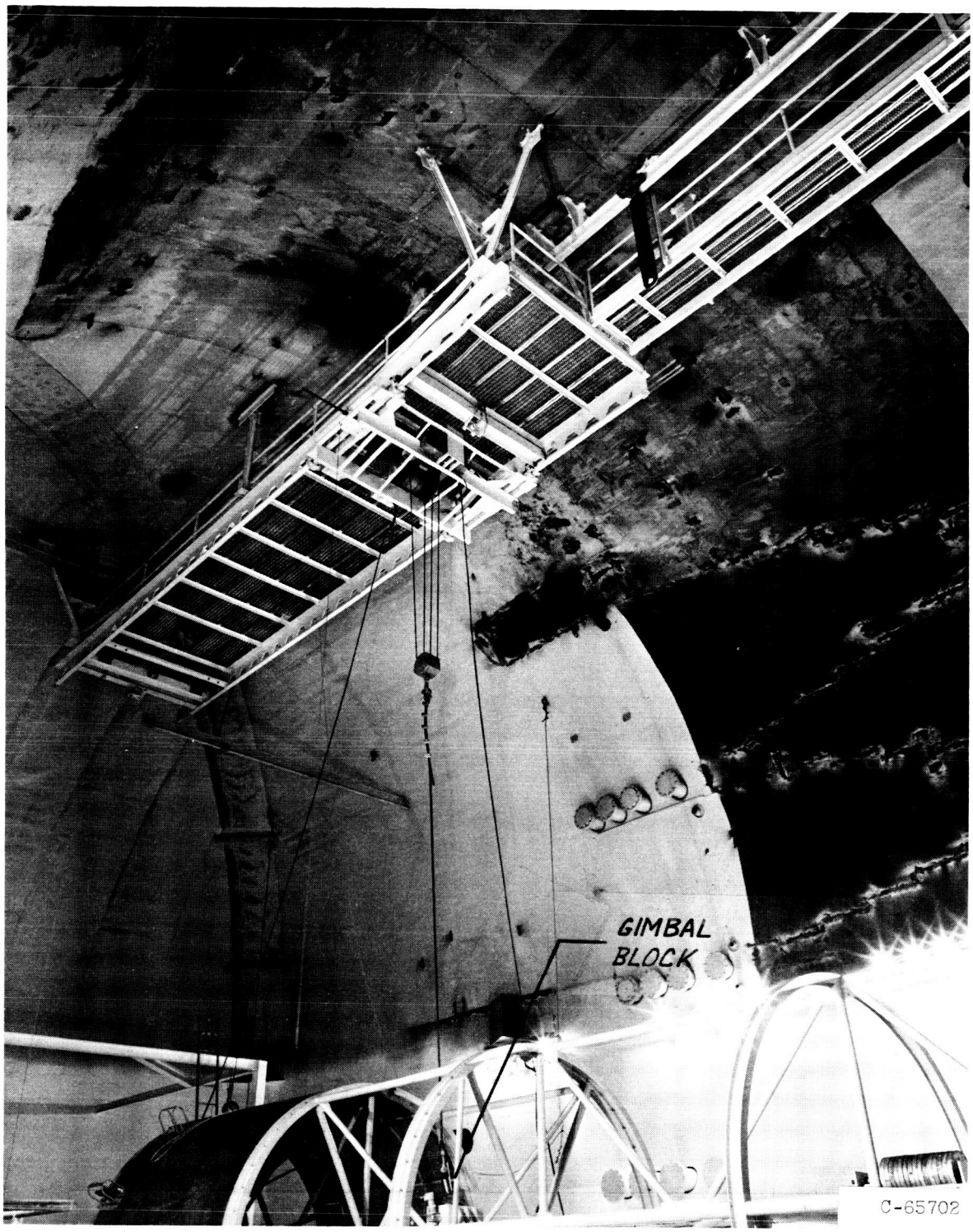

Figure 2. - Atlas suspension trolley and rails.

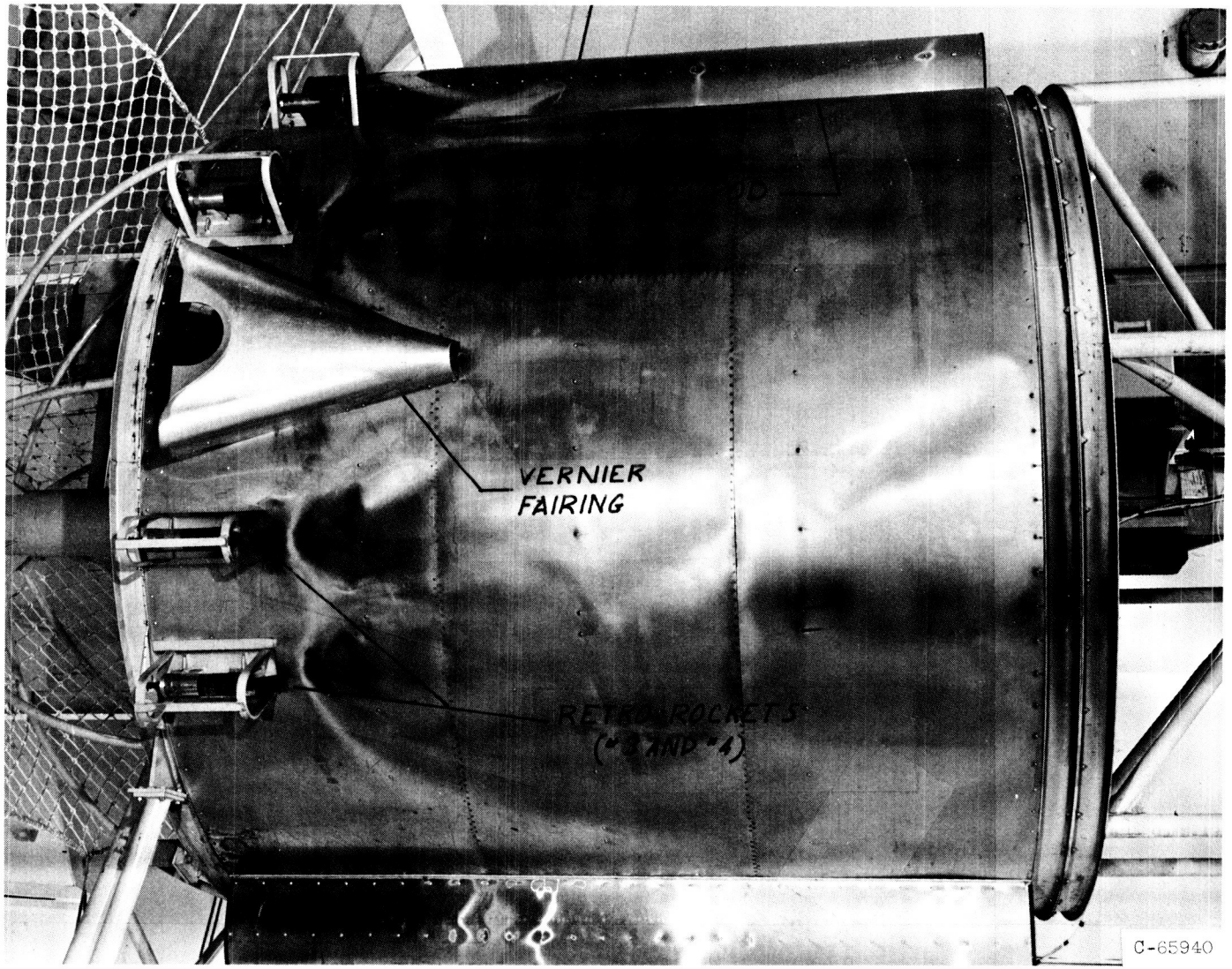

Figure 3. - Atlas model aft skin section.

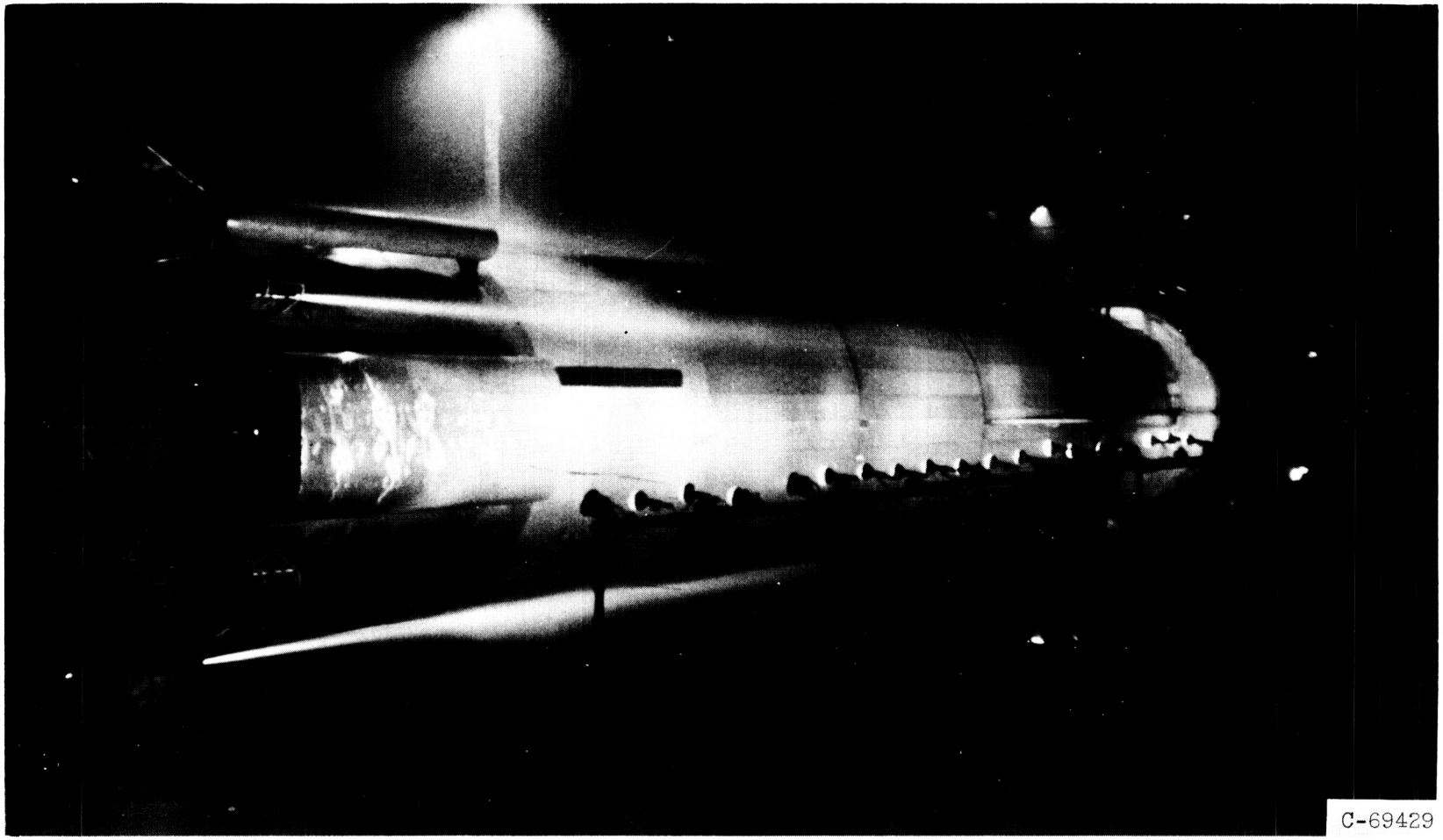

Figure 4. - Atlas model with rockets completing their burn cycle.

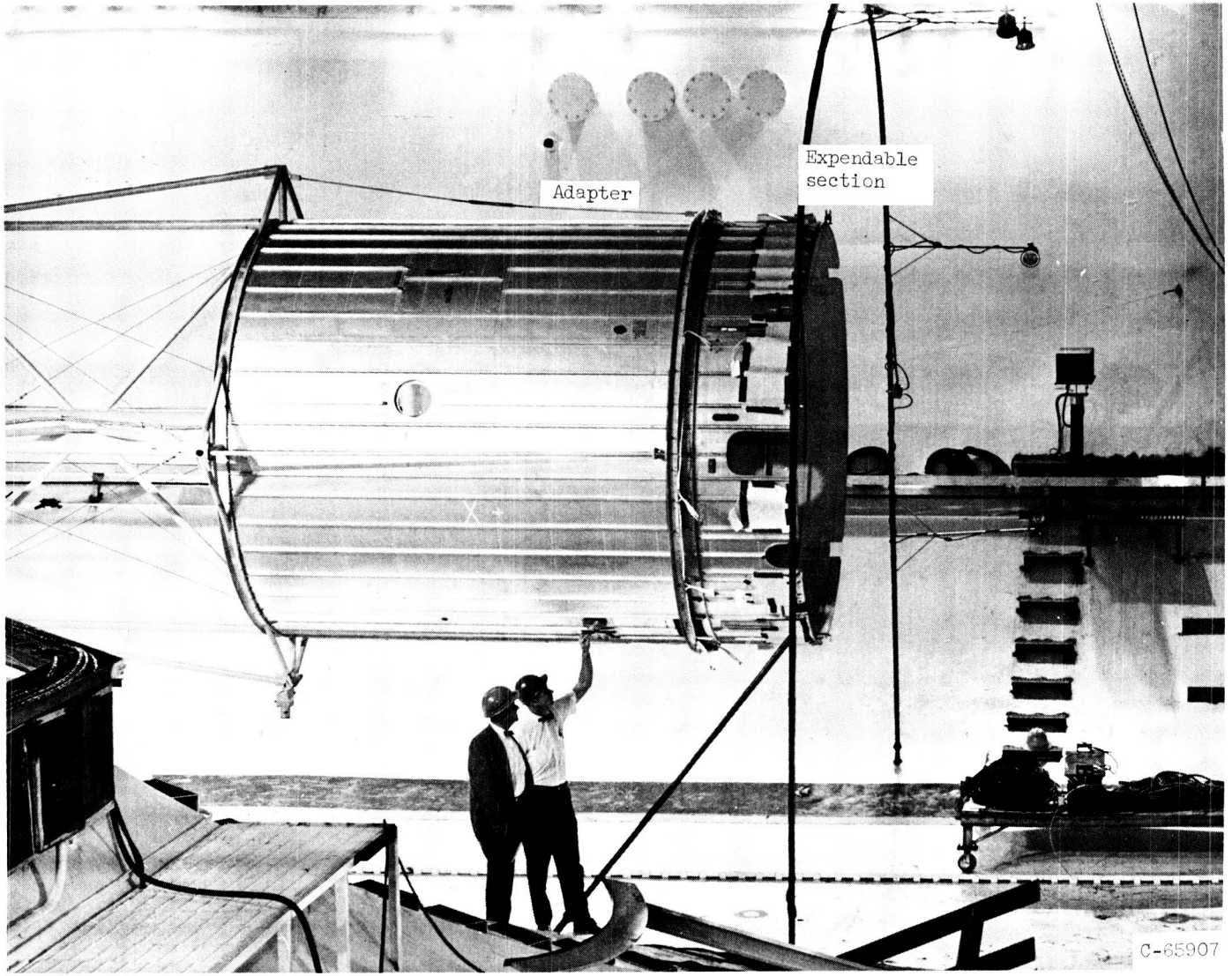

Figure 5. - Atlas model interstage adpater section.

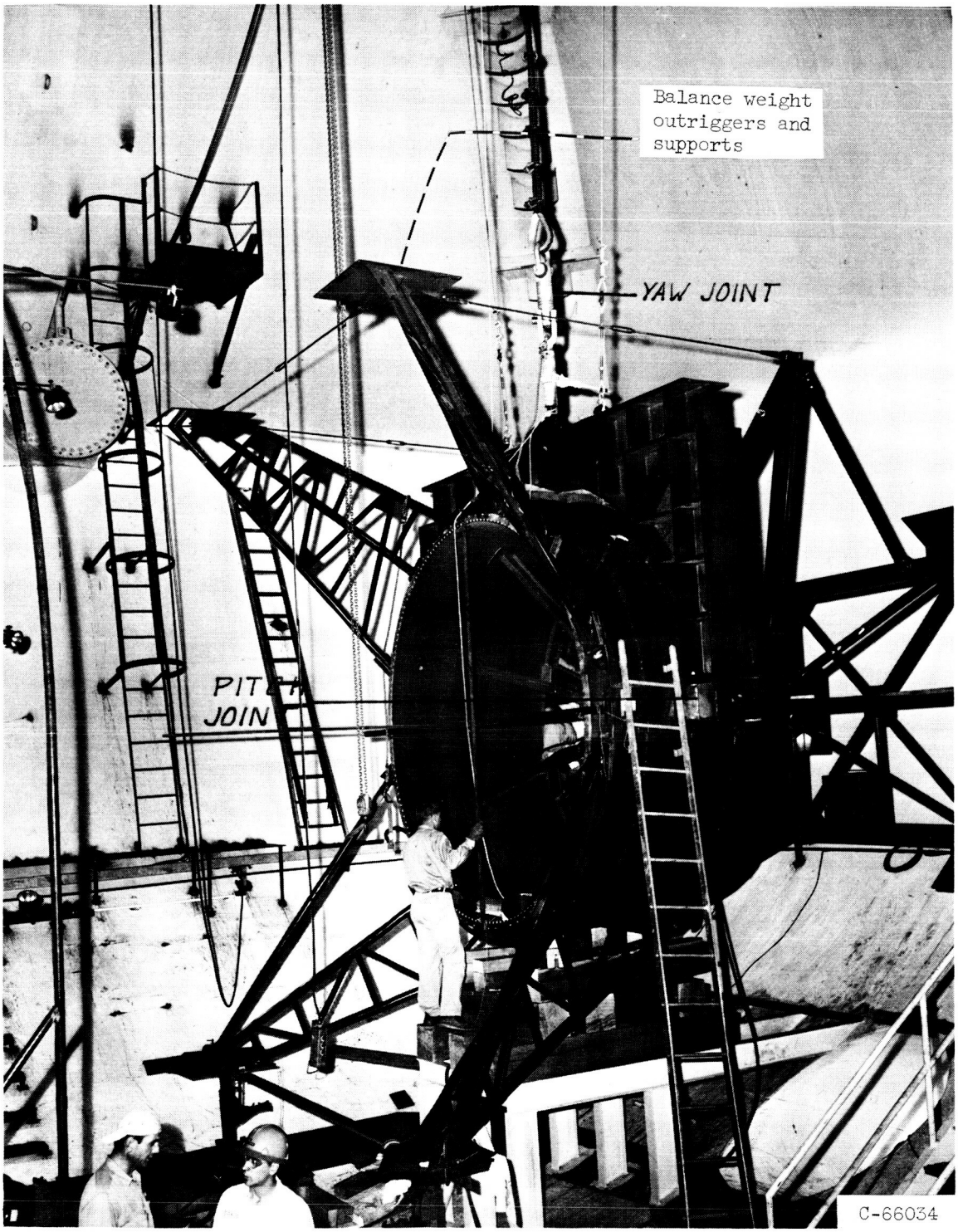

Figure 6. - Centaur model suspension joints.

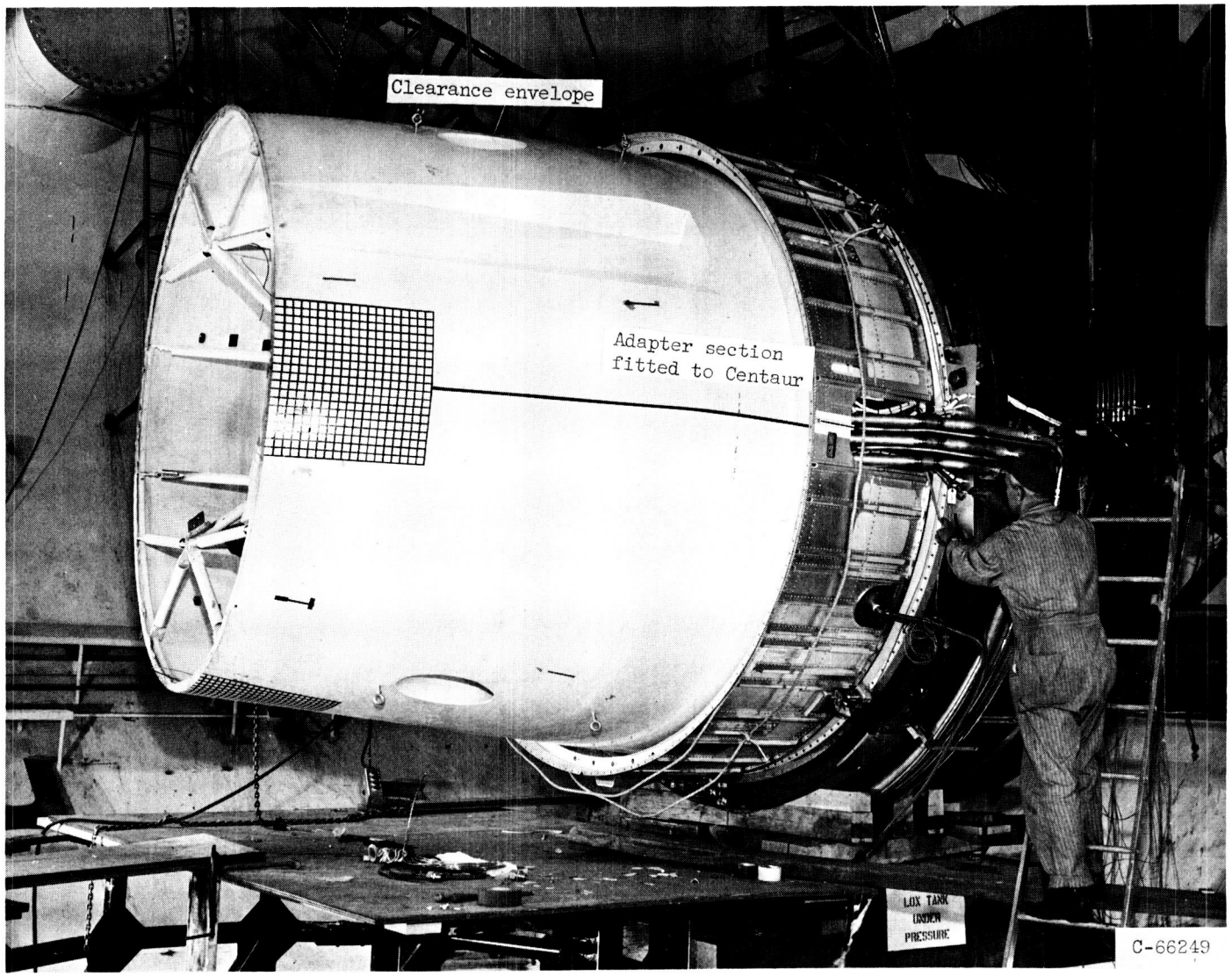

Figure 7. - Centaur model clearance envelope.

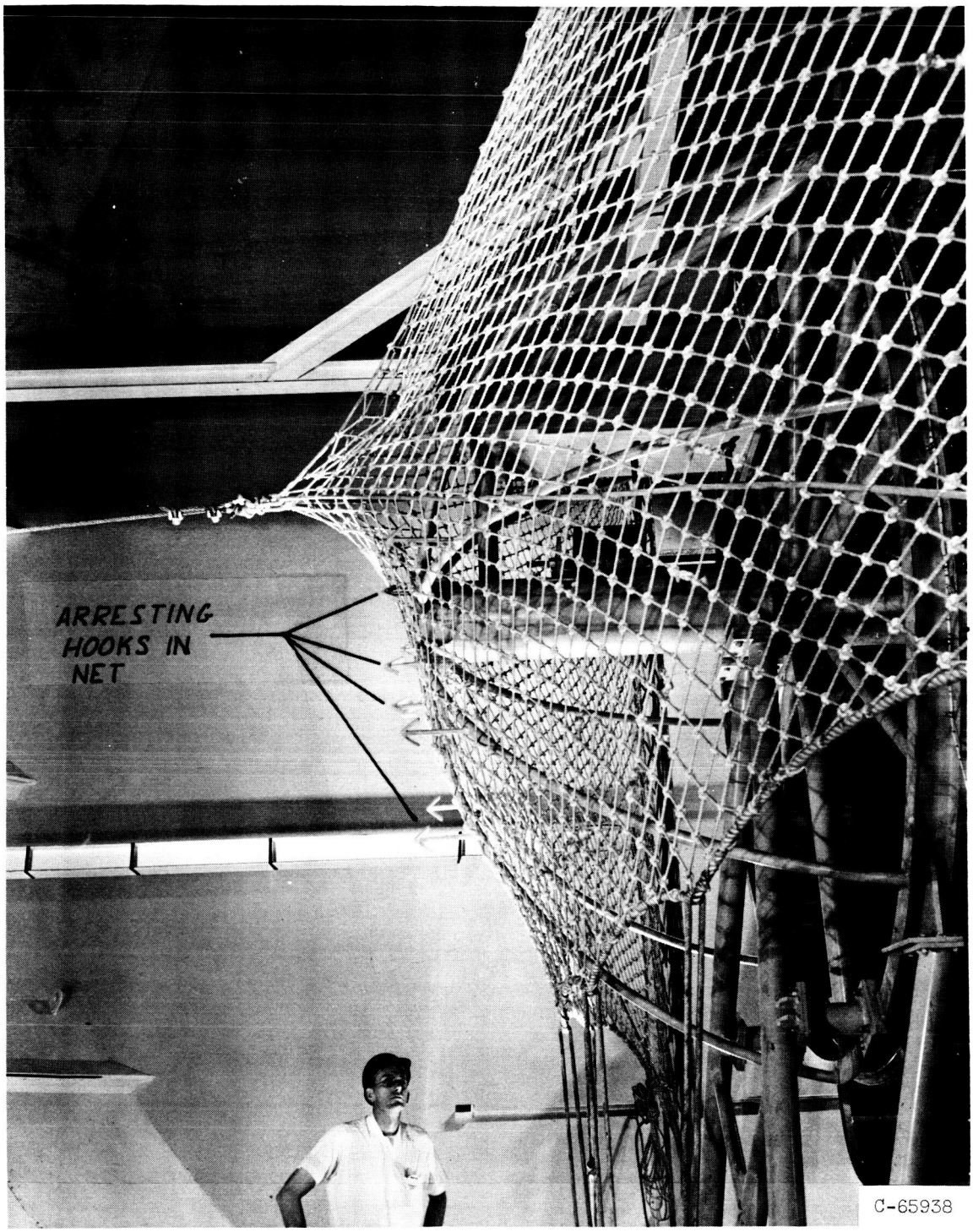

Figure 8. - Atlas model in arresting net.

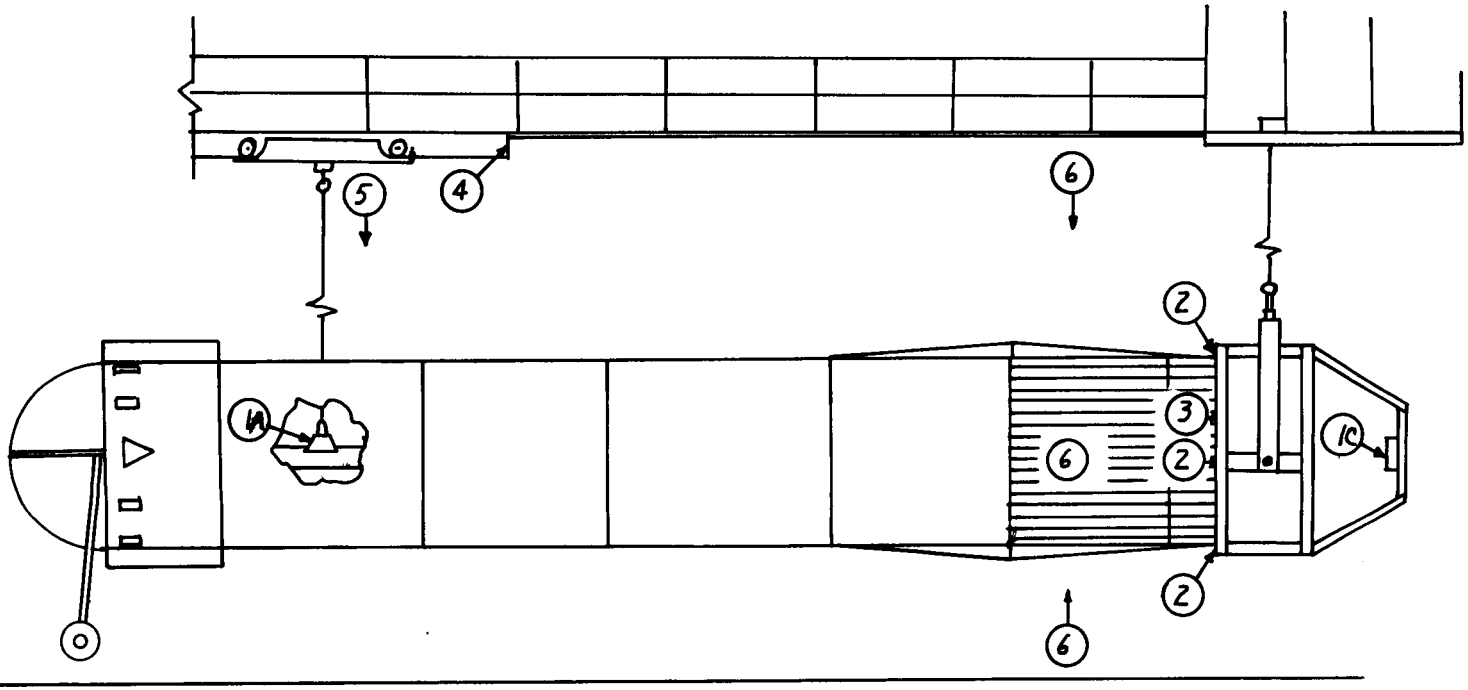

LEGEND:

1. ATLAS & CENTAUR RATE GYROS
2. FINE RANGE (2') EXTENSOMETERS 90° APART READING ATLAS LONG. DISPLACEMENT
3. COARSE RANGE (17') EXTENSOMETER READING ATLAS LONG. DISPLACEMENT
4. COARSE RANGE (17') EXTENSOMETER READING TROLLEY LONG. DISPLACEMENT
5. CAMERA ON TROLLEY SEEING ATLAS & TROLLEY MISALIGNMENT
6. CAMERAS SPACED 90° APART SEEING INTERSTAGE ADAPTER & CENTAUR CLEARANCE ENVELOPE MOTION

FIGURE 9. - SEPARATION TEST INSTRUMENTATION PLACEMENT

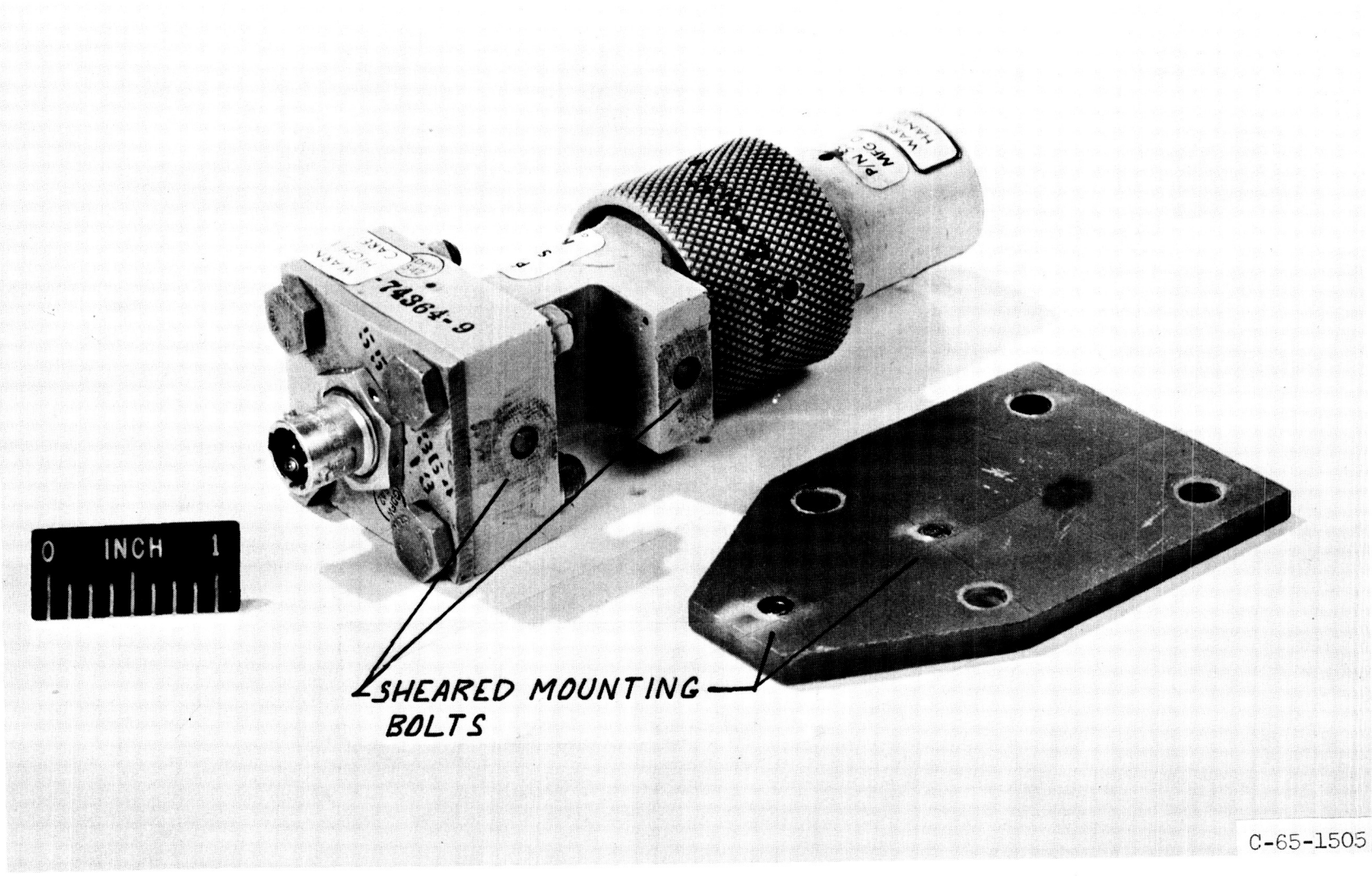

Figure 10. - Damaged AC-6 shaped charge detonator.

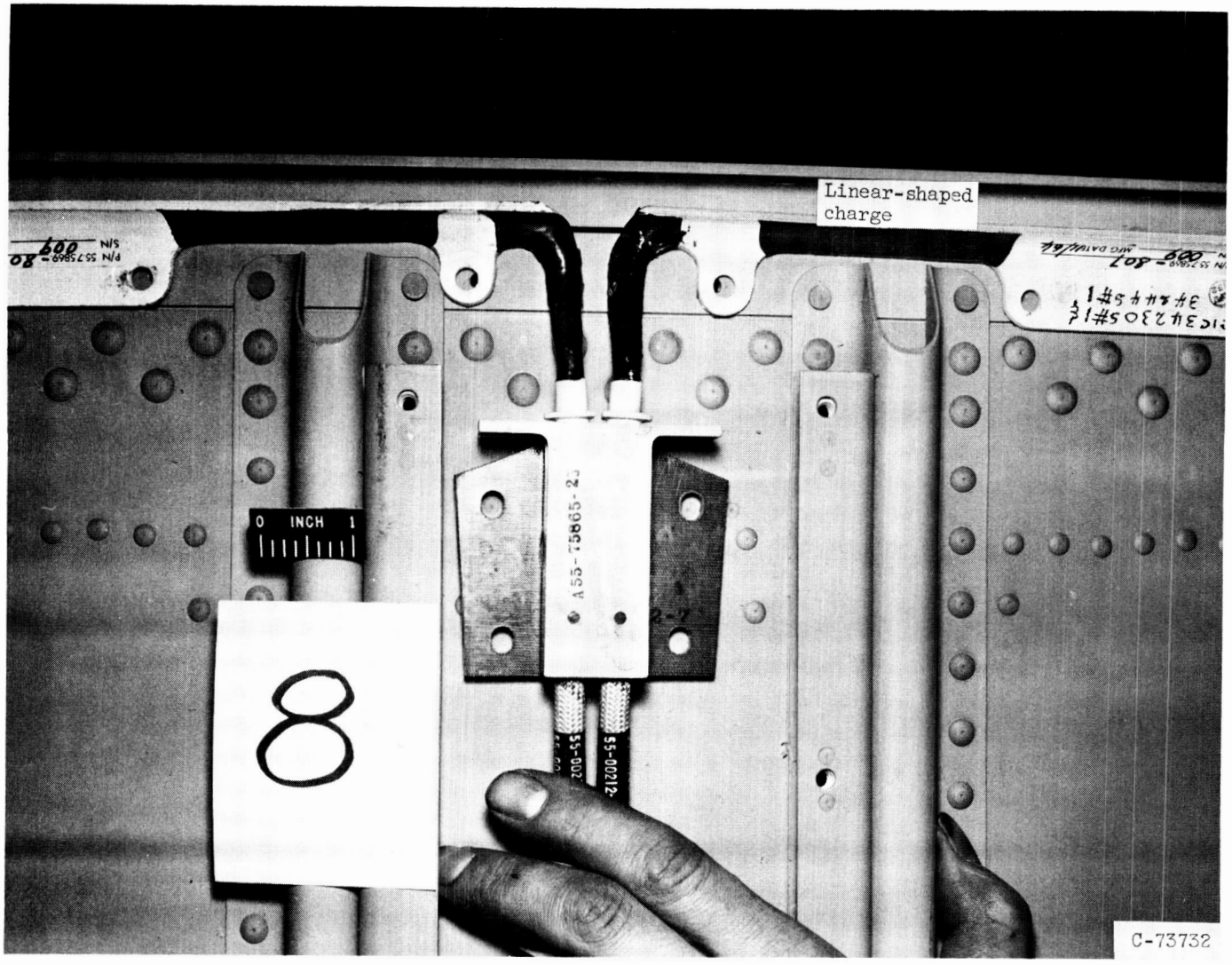

Figure 11. - Detonation transfer block as used on AC-6.

(a) Prior to test.

(b) Linear-shaped charge.

(c) Rocket ignition.

(d) Steady state turning.

(e) Beginning of rocket burnout.

(f) Rocket tail-off.

Figure 12. - Staging pyrotechnic sequence.

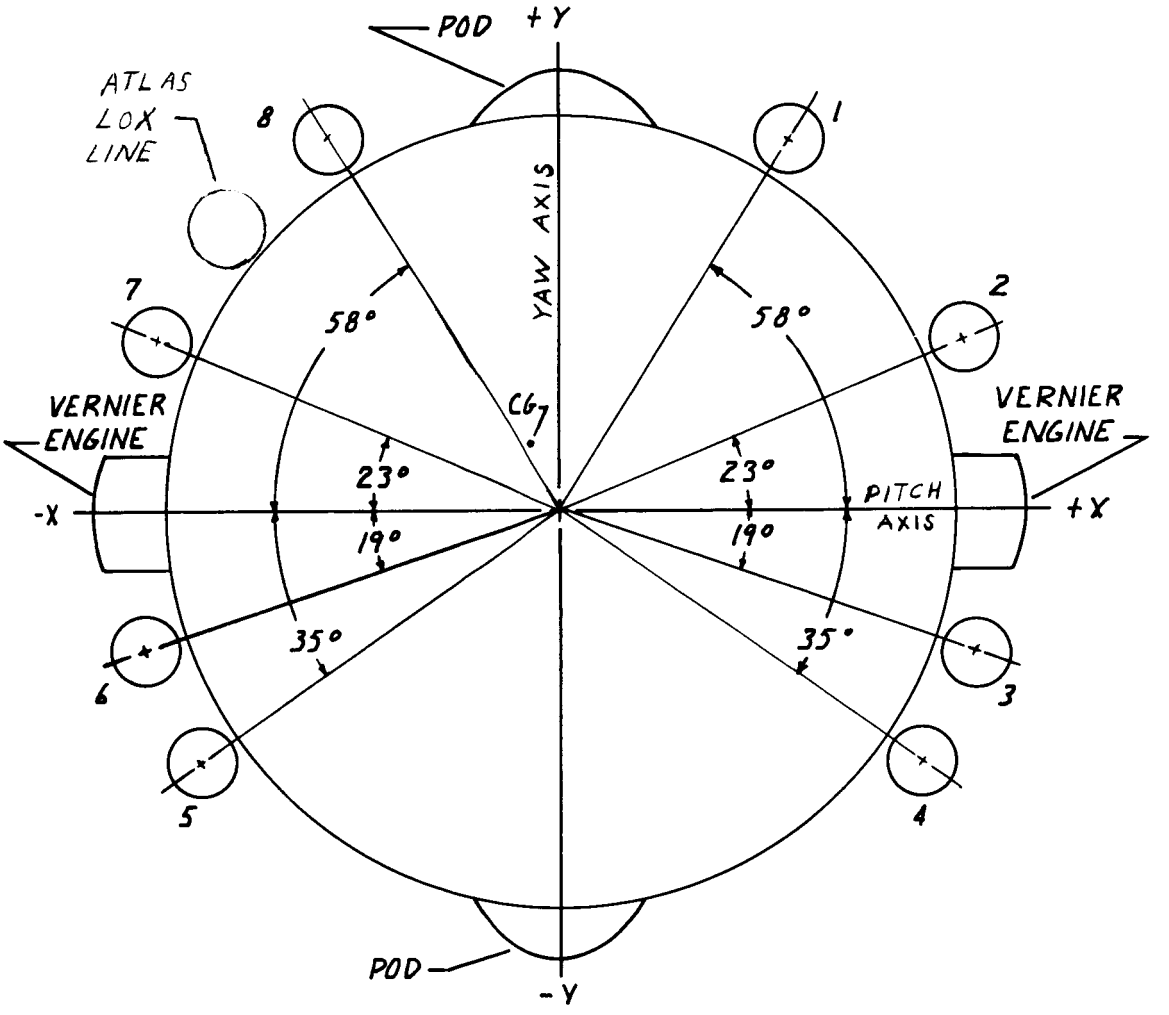

Figure 13. - ATLAS RETRO-ROCKET PLACEMENT AS SEEN FROM REAR

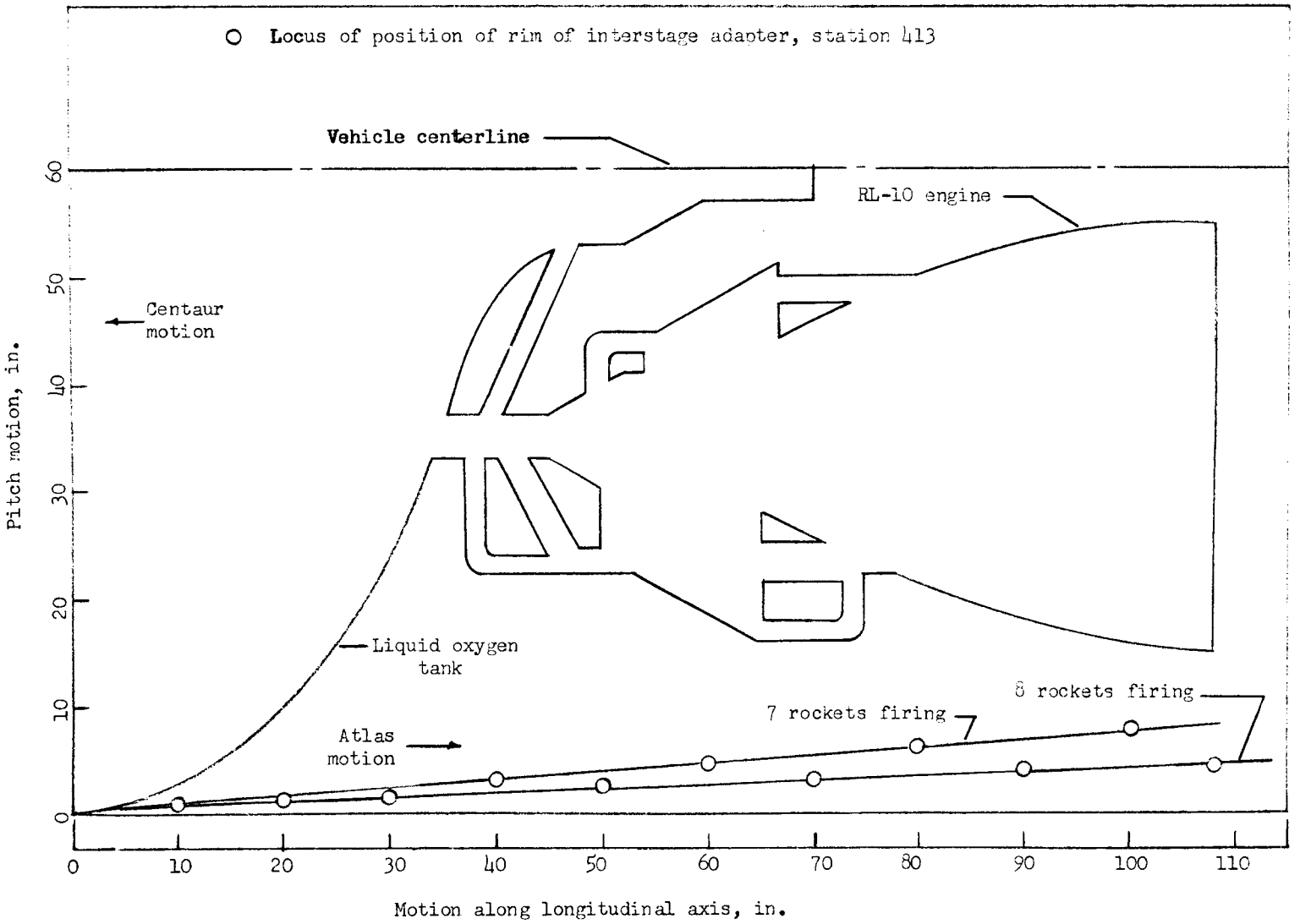

Figure 14 - Motion of station 413 on Atlas with respect to Centaur during staging

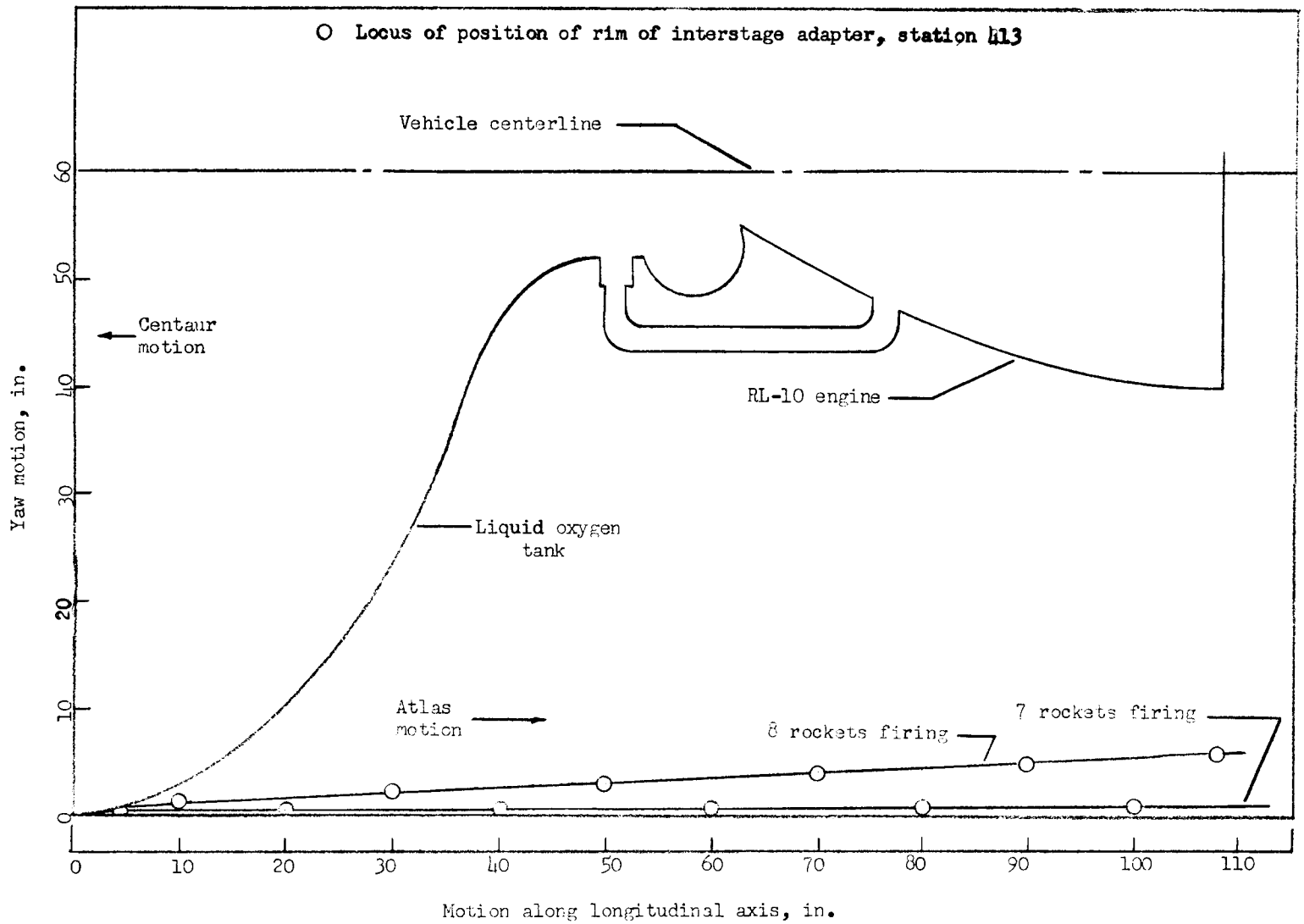

Figure 15 - Motion of station 413 on Atlas with respect to Centaur during staging

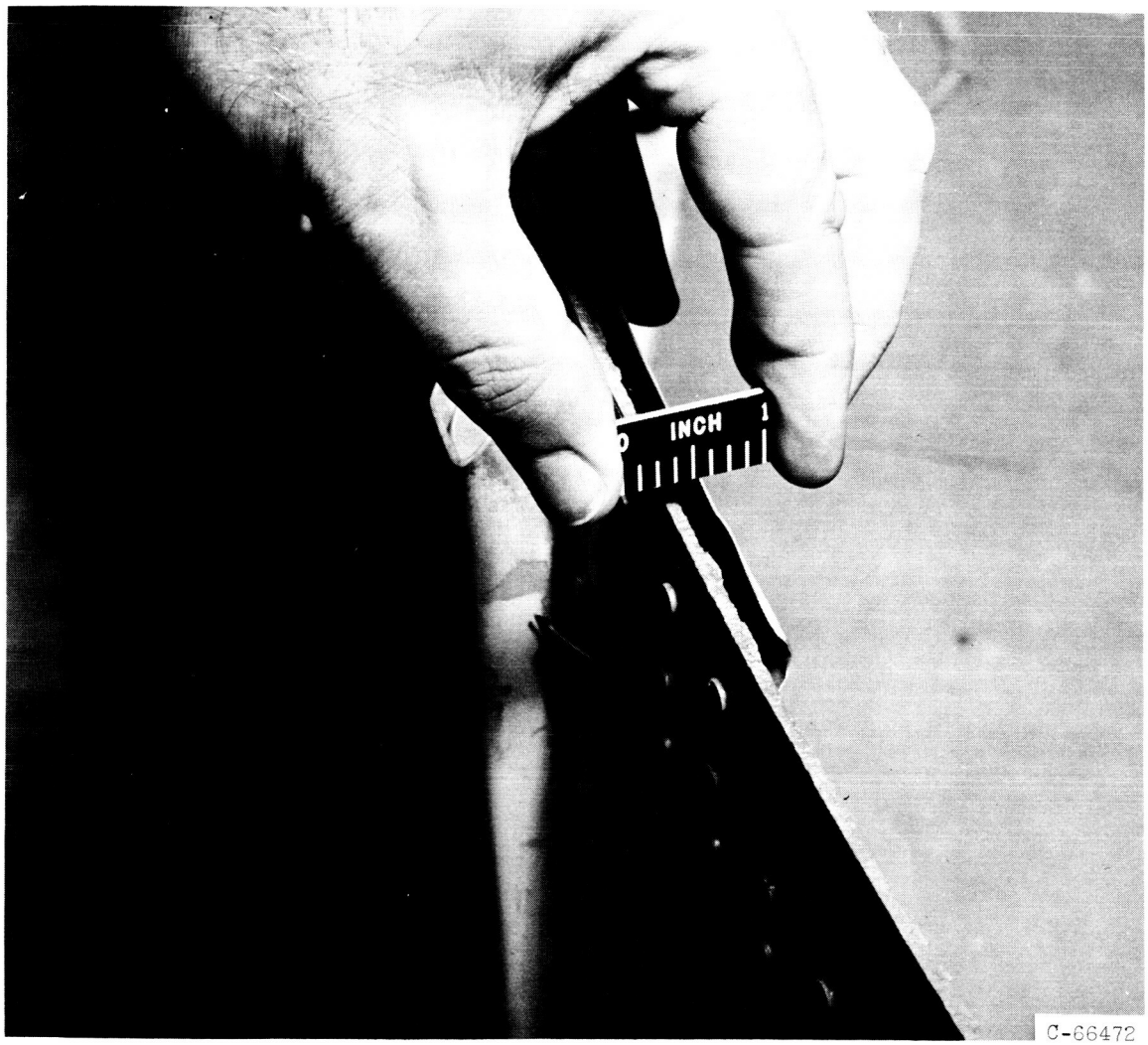

Figure 16. - Interstage adapter section cut by shaped charge.

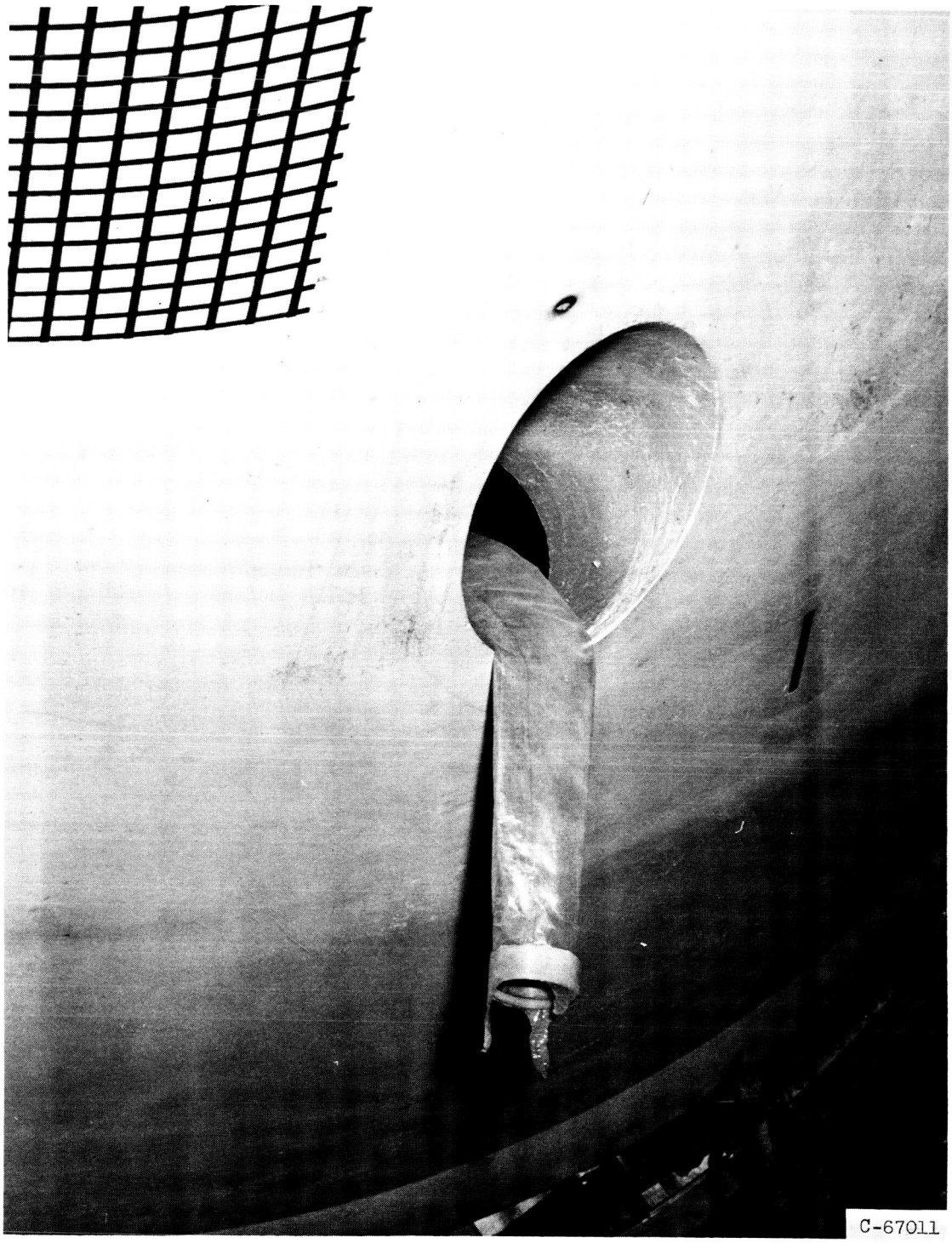

Figure 17. - Helium chill-down disconnect parted at secondary joint.

Figure 18. - Retrorocket fairing with cap that failed to eject.